P-ISSN 2586-9000
E-ISSN 2586-9027
Homepage : https://tci-thaijo.org/index.php/SciTechAsia
Science & Technology Asia
Vol. 26 No.4 October - December 2021
Page: [27-37]
*Original research article*

# Magnetic Field Effect on Lid-Driven Porous Cavity Heated to the Right Wall

A. Vanav Kumar[1,*], L. Jino[1,2], Swapnali Doley[1], M. Berlin[3]

[1]*Department of Basic and Applied Science, NIT Arunachal Pradesh, Arunachal Pradesh 791109, India*
[2]*Department of Automobile Engineering, Sathyabama University, Chennai 600119, India*
[3]*Department of Civil Engineering, NIT Arunachal Pradesh, Arunachal Pradesh 791109, India*

Received 20 August 2021; Received in revised form 21 November 2021
Accepted 27 November 2021; Available online 30 December 2021

**ABSTRACT**

In the present investigation, we report the behavior of magnetohydrodynamics mixed convective flow (MHD-MCF) of Cu-water nanofluid (Prandtl number, $Pr = 6.2$) inside a lid-driven porous square cavity is carried out. The hot temperature is applied on the right side of the cavity (wall). The governing equations are defined using continuity, momentum, and energy equations. Further, the continuity and momentum equations are transformed into a streamfunction-vorticity approach and solved using the finite difference method. The solutions are obtained through an implication of implicit scheme and successive under relaxation. The results of MHD-MCF within a cavity are represented by using the streamfunction ($\psi$), isotherms ($\theta$) and heatfunction ($\Pi$) for various values of Darcy number $10^{-2} \le Da \le 10^{2}$, Reynolds number ($1 \le Re \le 10$) and Hartmann number ($0 \le Ha \le 50$) at a fixed solid volume fraction ($\phi = 0.1$). An improvement in convective flow circulation is noticed on higher values of the Darcy number. Also, free convective effects are found to be prominent at lower $Re$ and forced convection effects make domination on higher $Re$

**Keywords:** Mixed field, Magnetic convection, Porous, Heatlines

## 1. Introducion

The necessity of heat transfer and fluid flow in porous media is increasing and advancing due to its huge variety of applications in the field of science, engineering, and technology. Some important applications for this type of problem are heat exchangers, separation processes in chemical industries, contaminant transport, geophysical problem, aquifer transport, etc. A comprehensive overview of the transport of fluids in porous media can be found in [1, 2]. Also, Applications of convection in porous media are found in [3-5]. In the past few years, the blending of nano-sized particles to the nor-

***Corresponding author:** vanavkumar.a@gmail.com **doi:** 10.14456/scitechasia.2021.63

mal to the normal conventional fluid is emerging due to its eligibility of increasing the overall thermophysical properties of the fluids [6, 7]. For instance, Sumit Gupta et al. [8] considered Ag/TiO2-water based nanofluids to pass over the vertical stretching sheet and analyzed the MHD free convective flows (MHD-FCF). Moreover, Sumit Gupta et al. [9] explored the heat/mass transfer of Cu-water and Al2O3-water nanofluid due to radiative MHD convective flow over an exponentially stretching surface. Recently, Jino and Vanav [10] examined the heat transfer and fluid flow (HTFF) within a Cu-$Al_2O_3$-water nanofluid packed porous cavity due to MHD-FCF. From the above studies, it is noticed that the heat transfer rate is increased by the nanofluids. In addition, Cu nanoparticle is found to actively improve the heat transfer performance over the other nanoparticles.

An impact of magnetic field effect in free convection on $Al_2O_3$-water nanofluid-filled square cavity is discussed by Ghasemi et al. [11]. It is noticed that the augmentation in $Ha$ makes areduction in the convective HTFF. Selimefendigil and Öztop [12] explored the MHD-FCF and its entropy generation inside a square enclosure with different shaped obstacles present inside. Selimefendigil et al. [13] later discussed in detail about the MHD-MCF and generation of the entropy in a cavity-filled nanofluid. Basak et al. [14-16] analyzed the effect of mixed convective HTFF in a lid-driven square-shaped cavity with various types of boundary conditions. From their studies, it is observed that the heat transfer increases by augmenting the Darcy number and Grashof number. An increase in Reynolds number leads to forced convection to be dominant. Also, the flow intensity improved with the increase in Darcy number. Emami et al. [17] investigated the free convection effects on HTFF in an inclined porous cavity filled with Cu-water nanofluid. The study concludes that every parameter involved in the study such as inclination angle, $Da, Ra$ and $\phi$ holds the responsibility in HTFF.

Wilkes [18] explained the finite difference computations (FDC) to solve the FCF within a rectangular cavity. Moreover, Rudriah et al. [19] extended the FCF to MHD-FCF within a cavity by using FDC. Recently, Jino and Vanav [20] used FDC to solve the MHD-FCF in a Cu-water nanofluid-packed porous enclosure. Other than the FDC techniques, Jagdev Singh et al. [21, 22] used hybrid methods such as homotopy perturbation Elzaki/homotopy analysis transform to solve the non-linear equations to interpret the fluid flow. Also, Sumit Gupta et al. [23] considered Homotopy analysis to determine the analytical solution to interpret the nanofluid flow over the variable thickness surfaces due to radiative MHD flows.

Grosan et al. [24] discussed the HTFF within a porous enclosure on MHD-FCF and heat generation effect. Revnic et al. [25] discussed the unsteady natural convective flow in a porous cavity. The study apprises that the diffusive heat transfer becomes prominent when increasing the $Ha$ and $Ra$. Rashad et al. [26] analyzed the internal heat generation and MHD-FCF within a rectangular enclosure that is filled with Cu-water nanofluid. The result highlights that the heat transfer increases with $\phi$. Also, when advancing $Ha$, the maximum valus of the temperature enhaces and streamfucniton intensity decreases. Jino et al. [27-31] discussed the MHD-FCF in a porous square cavity filled with Cu-water nanofluid. The porous media is framed using the Carman-Kozeny/Darcy-Brinkman equations. The studies are discussed with various thermal boundaries. Also, heatfunction visualization was incorporated for better prediction of heat flow. From the studies, it is noted that the heatfunction study is indispensable for understanding the heat flow. In addition, it is noted that the Cu-water nanofluid involves in enhancement in the heat transfer process. Sivasankaran et al. [32] numerically studied

the MCF in a lid-driven porous cavity containing Cu-water nanofluid by considering a partial slip. Chamkha et al. [33] discussed the effect of source-sink on MHD-MCF within a lid-driven porous cavity. Chamkha et al. [33] investigated the MHD-MCF within a porous lid-driven cavity. It is noted that the addition of Cu nanoparticles enhances entropy generation. Sheikholeslami [34] discussed nanofluids' MHD-MCF in a lid-driven porous cavity. The results denote that the effect of convective heat transfer increases for an increase in $Da$ and $Re$. Also, it is noted that the heat transfer declines with $Ha$. Çolak et al. [35] explored the HTFF due to convection and partially heated block within a cavity. The results show that the heat transfer is drastically increasing on higher $Da$ as well as with the orientation in the heater block.

The present study illustrates the MHD-MCF on the lid-driven porous enclosure of square-shaped. The Cu-water nanofluid's HTFF is discussed by using the flow contour visualization tools such as streamlines, heatlines, and isotherms. The role of $Ha$, $Da$ and $Re$ in flow characteristics by heating the right side of the cavity are demonstrated.

## 2. Problem Description

The two-dimensional square cavity of side distance $H \times H$, filled up with the Cu-water nanofluid is considered. The properties of the loaded nanofluid (base fluid and nanoparticle) are given in Table 1.

The velocities $u$ and $v$ are considered along the horizontal direction $x$ and vertical direction $y$. The right side of the cavity is maintained at higher temperature ($T_h$), ($T_c$) left wall is maintained at a lower temperature ($T_c$) and the other two walls are adiabatic respectively. The top wall of the cavity is moving with the uniform velocity ($u = U_0$) and other walls are maintained stationary as shown in the Fig. 1.

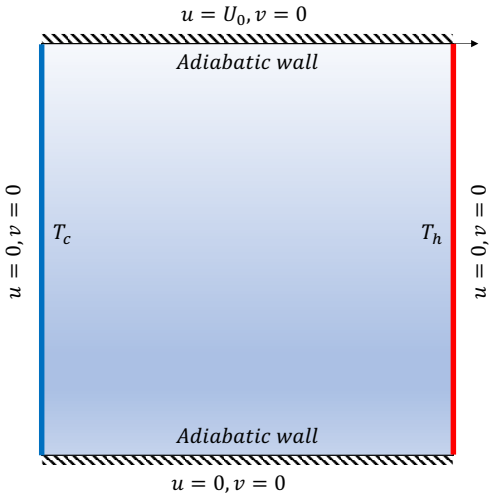


**Fig. 1.** Problem model.

**Table 1.** Physical properties.

| | Water | Cu particle |
|---|---|---|
| $\rho\ (kg/m^3)$ | 997.1 | 8933 |
| $\mu\ (Pa\ s)$ | $8.9\times10^{-4}$ | – |
| $c_p\ (J/kg\ K)$ | 4179 | 385 |
| $k\ (W/m\ K)$ | 0.613 | 401 |
| $\sigma\ (S/m)$ | 0.05 | $5.96\times10^{7}$ |
| $\beta\ (K^{-1})$ | $2.1\times10^{-4}$ | $16.7\times10^{-4}$ |

The Boussinesq approximation is applicable for fluid properties and the other properties are maintained constant. By the assumptions made, the governing equations for flow in a cavity are given by,

$$\frac{\partial u}{\partial x}+\frac{\partial v}{\partial y}=0 \tag{2.1}$$

$$\rho_n\left[u\frac{\partial u}{\partial x}+v\frac{\partial v}{\partial y}\right]=\mu_n\left(\frac{\partial^2 u}{\partial x^2}+\frac{\partial^2 v}{\partial y^2}-u\frac{\mu_n}{K}\right)-\frac{\partial p}{\partial x} \tag{2.2}$$

$$\rho_n\left[u\frac{\partial u}{\partial x}+v\frac{\partial v}{\partial y}\right]=\mu_n\left(\frac{\partial^2 u}{\partial x^2}+\frac{\partial^2 v}{\partial y^2}-v\frac{\mu_n}{K}\right)-\frac{\partial p}{\partial y}+(\rho\beta)_n g(T_h-T_c)-\sigma_n B_0^2 v \tag{2.3}$$

$$\left(\rho c_p\right)_n\left[u\frac{\partial T}{\partial x}+v\frac{\partial T}{\partial y}\right]=k_n\left(\frac{\partial^2 T}{\partial x^2}+\frac{\partial^2 T}{\partial y^2}\right) \tag{2.4}$$

where the thermophysical properties are the function of solid volume fraction is given by,

$$\mu_n=\mu_f/(1-\phi)^{2.5} \tag{2.5}$$

$$\mu_n=\mu_f/(1-\phi)\rho_f+\phi\rho_p \tag{2.6}$$

$$\left(\rho c_p\right)_n=(1-\phi)\left(\rho c_p\right)_f+\phi\left(\rho c_p\right)_p \tag{2.7}$$

$$\left(\rho\beta\right)_n=(1-\phi)\left(\rho\beta\right)_f+\phi\left(\rho\beta\right)_p \tag{2.8}$$

$$k_n=k_{fl}\left[\frac{k_p+2k_f-2\phi\left(k_f-k_p\right)}{k_p+2k_f-2\phi\left(k_f-k_p\right)}\right] \tag{2.9}$$

Also, the velocities $(u,v)$, pressure $(p)$ and temperature $(T)$ are the function of two-dimensional space $x$ and $y$, respectively.

The above dimensional governing Eqs. (2.1-2.4) can be non-dimensionalized using the parameters,

$$U=\frac{u}{U_0},\qquad V=\frac{v}{U_0},$$

$$X=\frac{x}{H},\qquad Y=\frac{y}{H},$$

$$P=\frac{p}{\rho_f U_0^2},\qquad \theta=\frac{T-T_c}{T_h-T_c},$$

$$Pr=\frac{\nu_f}{\alpha_f},\qquad Re=\frac{U_0 H}{\nu_f},$$

$$Da=\frac{k}{H^2},\qquad Ha=B_0 H\sqrt{\frac{\sigma_f}{\rho_f\nu_f}},$$

$$Gr=\frac{g\beta_f H^3(T_h-T_c)}{\nu_f^2}.$$

The dimensionless flow equations thus derived after the substitution of the above non-dimensional parameter to the primary two-dimensional Eqs. (2.1-2.4) as,

$$\frac{\partial U}{\partial X}+\frac{\partial V}{\partial Y}=0 \tag{2.10}$$

$$U\frac{\partial U}{\partial X}+V\frac{\partial V}{\partial Y}=\frac{\mu_n\rho_f}{\rho_n\mu_f}\cdot\frac{1}{Re}\left(\frac{\partial^2 U}{\partial X^2}+\frac{\partial^2 U}{\partial Y^2}-\frac{U}{Da}\right)-\frac{\rho_f}{\rho_n}\cdot\frac{\partial P}{\partial X} \tag{2.11}$$

$$U\frac{\partial V}{\partial X}+V\frac{\partial V}{\partial Y}=\frac{\mu_n\rho_f}{\rho_n\mu_f}\cdot\frac{1}{Re}\left(\frac{\partial^2 V}{\partial X^2}+\frac{\partial^2 V}{\partial Y^2}-\frac{V}{Da}\right)-\frac{\rho_f}{\rho_n}\cdot\frac{\partial P}{\partial Y}+\frac{(\rho\beta)_n}{\rho_n\beta_f}\cdot\frac{Gr}{Re^2}\theta-\frac{\rho_f\sigma_n}{\rho_n\sigma_f}\cdot\frac{Ha^2}{Re}V \tag{2.12}$$

$$U\frac{\partial\theta}{\partial X}+V\frac{\partial\theta}{\partial Y}=\frac{\alpha_n}{\alpha_f}\left(\frac{\partial^2\theta}{\partial X^2}+\frac{\partial^2\theta}{\partial Y^2}\right) \tag{2.13}$$

The pertinent dimensionless flow equations are solved using the thermal boundaries as $\theta=1$ at the left wall, $\theta=0$ at the right wall, and $\partial\theta/\partial Y=0$ at the horizontal wall. Top lid movement, $U_0=1,\ V=0$ and remaining wall velocities as $U=0,\ V=0$.

Streamline-$\psi$ and heatlines-$\Pi$ are adopted for better picturization of the fluid and heat flow respectively.

$$\frac{\partial^2\psi}{\partial X^2}+\frac{\partial^2\psi}{\partial Y^2}=\frac{\partial U}{\partial Y}-\frac{\partial V}{\partial X} \tag{2.14}$$

$$\frac{\partial^2 \Pi}{\partial X^2}+\frac{\partial^2 \Pi}{\partial Y^2}=\frac{\partial(U\theta)}{\partial Y}-\frac{\partial(\mathrm{V}\theta)}{\partial X} \qquad (2.15)$$

Local Nusselt number is used to represent the transfer of heat from the right wall and it is given by,

$$Nu=\frac{k_n}{k_f}\cdot\left.\frac{\partial\theta}{\partial X}\right|_{wall} \qquad (16)$$

## 3. Numerical Solution

Governing Eqs. (2.1-2.4) are non-dimensionalized (2.10-2.13) and, the continuity and momentum equations are formulated into the vorticity-streamfunction based equations. Further, the equations are solved by using the implicit-FDC. The computation is carried out still the residuals for the streamfunction get below $10^{-5}$.

The work is initiated after validating the code with a previously published work. Fig. 2 shows a good comparison between the results by Basak et al. [10] and the present study.

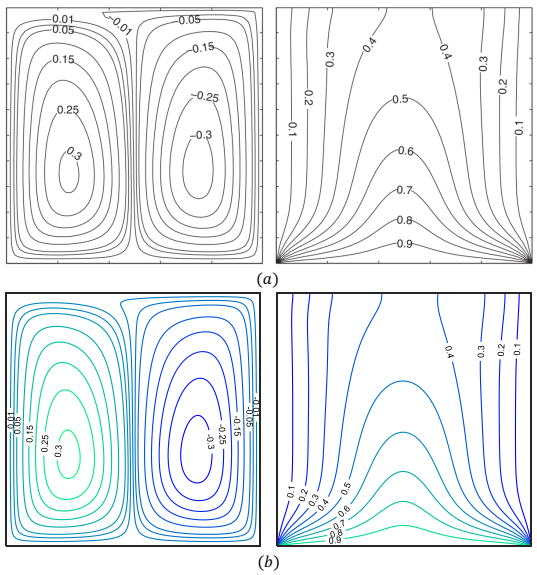

**Fig. 2.** Validation of $\psi$ and $\theta$ with the earlier studies.

## 4. Result and Discussions

The HTFF of lid-driven porous cavity due to the MHD-MCF on heated right wall is studied by varying the dimensionless parameters such as Darcy number $\left(10^{-2}\le Da\le 10^{2}\right)$, Hartmann number $\left(0\le Ha\le 50\right)$ and Reynolds number $(1\le Re\le 10)$. The whole computation is done for fixed parameters solid volume fraction $\left(\phi=0.1\right)$, Prandtl number $\left(Pr=6.2\right)$, and Grashof number $\left(Gr=10^{4}\right)$. The results are framed by using $\psi$, $\theta$ and $\Pi$ respectively. In addition, the heat transfer from the right wall is demonstrated using $Nu$.

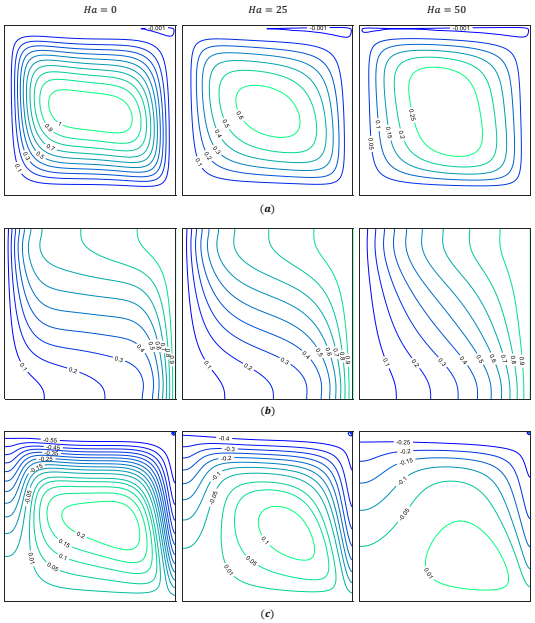


**Fig 3.** Streamfunction (a), Isotherms (b), Heatfunction (c) for various $Ha$ at $Da=10^{-2}$ and $Re=1$.

Fig. 3 represents (a). streamlines, (b). isotherms and (c). heatlines for various values of Hartmann number $\left(Ha=0,\ 25,\ 50\right)$ at $Da=10^{-2}$ and $Re=1$. When the $Ha$ equals $0$, there is primary circulation which covers the major region of the cavity. Also, a small secondary circulation arises adjacent to the right wall.

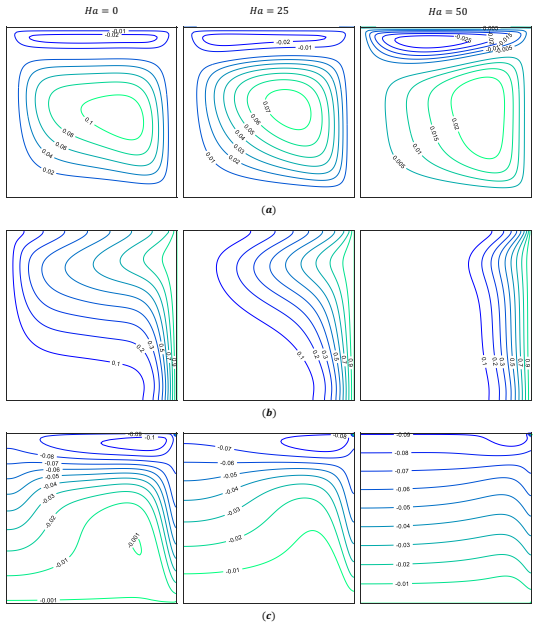


**Fig 4.** Streamfunction (a), Isotherms (b), Heatfunction (c) for various $Ha$ at $Da = 10^{-2}$ and $Re = 10$.

This secondary circulation at the top is due to the lid-driven effects. With respect to the $\psi$, the temperature is distributed from the heated wall. Moreover, the heat flow can be visualized clearly in the contour $\Pi$. The heat travels from the right wall to the left. The denser heatlines adjacent to the heated right wall and the circulation indicates the convective heat transfer. By the way, when $Ha$ increases to 25 and 50 it causes widening of $\psi$ contour from the horizontal direction to the vertical direction by reducing the intensity. In addition, the growth of secondary circulation is noted with the augmentation in the $Ha$, which is observed at the top of the cavity.

The increase in $Ha$ causes an increase in the applied magnetic field which is from the direction left to right. It is well-known fact that the magnetic field subdues the flow of fluid inside the cavity by the resistive force. At $Ha = 0$, the flow is free from any kind of magnetic force hence, the circulation of fluid is intense as seen from Streamlines of Fig. 3(a) (left). As $Ha$ increases, the circulation of fluid is less intense due to the suppressive act of an applied magnetic field. Hence, the contours represent the same in Fig. 3(a) (middle and right) as compared to Fig. 3(a) (middle). However, as the convective effects are getting weak (heatlines also represent the same), the fluid is replaced by a counter flow from the right corner as seen from Fig. 3(a)(right), which is also supported by the moving lid. This eventually is due to the conservation of mass law, which is the equation of continuity.

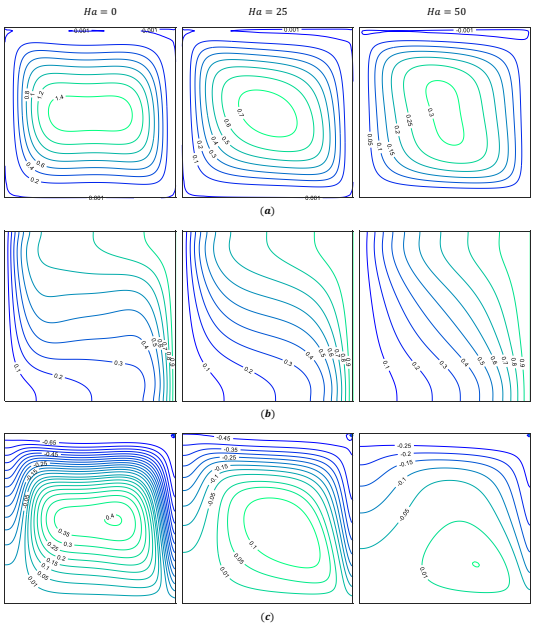


**Fig 5.** Streamfunction (a), Isotherms (b), Heatfunction (c) for $Ha$ at $Da = 10^{2}$ and $Re = 1$.

Similarly, Fig 4 represents the flow patterns for $Re = 10$. Here, the bottom primary circulation intensity is reduced as compared to Fig 3. Also, the secondary circulation has grown more than ten times. This is due to the action of forced convection. By increasing $Re$, the force from the lid drives the flow and thus rises the secondary circulation. Since the primary circulation is weaker than at the lower $Re$, temperature distribution over the entire cavity is affected. Moreover, only where the region between

both the circulations are met, where the temperature distribution is more. From the contour $\Pi$, it is clearly visible that the bottom heatline circulation is weaker as compared to the top secondary circulation. This illustrates the forced convective heat transfer than the natural convection. However, while $Ha = 50$ there is no circulation detected, and this signs the conductive dominated heat flow.

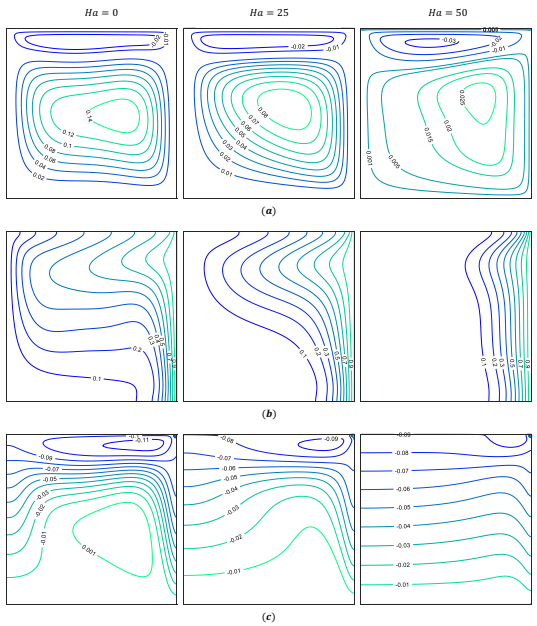


Fig 6. Streamfunction (a), Isotherms (b), Heatfunction (c) for various $Ha$ at $Da = 10^2$ and $Re = 10$.

Fig. 5 represents the flow field for various $Ha$ at $Da = 10^2$ and $Re = 1$. At $Da = 10^2$, the contours of $\psi$, $\theta$ and $\Pi$ are looks similar as in the case of $Da = 10^{-2}$. However, the intensity of streamfunction increases due to the increase in permeability. This leads to augmentation in the buoyancy effect than the viscous force. The intense flow causes the temperature to distribute all over the cavity and increases the convective heat transfer rate. In the absence of a magnetic field effect, the heatline circulation intensity is much higher and denser lines are observed adjacent to the right wall. In addition, no secondary circulations are noted. This leads us to conclude the domination of the free convective heat transfer regime. This FCF gets destroyed by the action of augmenting $Ha$. This can be noticed in the heatline plots (reduced denser lines and circulations) on $Ha = 25$ and 50. Meanwhile, in Fig. 6, it is noticed that the increase in $Re$ to 10 also increases overall flow intensity as compared to the lower Darcy number $\left(Da = 10^{-2}\right)$. Because of the increased permeability and forced convective behavior, overall secondary circulation intensity is raised.

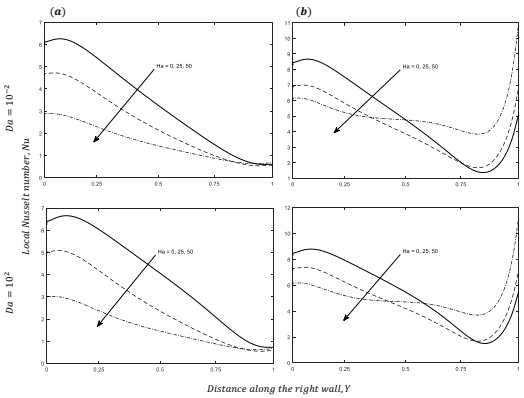


**Fig. 7.** Visualization of local Nusselt number.

Heat transfer originates along the right wall is denoted by local Nusselt number, which is presented in Fig 7. At lesser $Re$, a lower portion of the right wall provides the highest heat transfer rate and gradually decreases towards the top of the wall. A very small variation in $Nu$ due to the lid movement effect is noted in the case of $Re = 1$. This $Nu$ reduces by increasing the Hartmann number because of the resistive force generated in the flow and this leads a viscous force to slow down the convective heat transfer rate. But for the higher $Re$, the local Nusselt number decreases from the lower region of the right wall till $3/4^{th}$ of the cavity and increases further. Heat transfer due to lid movement (FCF) increases by quantifying the Reynolds number. At $Re = 10$, the

transfer of heat decreases at bottom of the wall and increases at the top while quantifying the $Ha$ . At the same time, the non-existence of a heatline circulation at the upper side cavity on higher $Ha$ indicates the improvement in the conduction-based heat transfer.

## 5. Conclusion

The MCF in a porous lid-driven square cavity is studied by considering higher temperatures on the right wall. The study is addressed with the effects of a magnetic field. Some of the main observations are,

- Fluid velocity augments with permeability by advancing the Darcy number from $10^{-2}$ to $10^{2}$.
- An improvement in $Ha$ leads to reducing the heatline and streamline circulations.
- Forced convective HTFF increases with increasing the $Re$.
- Circulations at the primary circulation (lower) are due to free convection and the top secondary circulation is due to forced convection.
- This study shows that heatline plots are indispensable for heat flow analysis and give a fine insight into the HTFF.
- At $Re = 10$, an increase in $Ha$ causes no circulation in the heatlines. This illustrates the conduction mode of heat transfer.

Apart from this study, the authors would like to suggest future research directions. Some suggestions are,

- The different types of nanofluid can be explored. Further, the hybrid nanofluids flow has to be explored deeply.
- Exergy analysis has to be performed on various nanofluid/hybrid nanofluids flow.
- Since lesser research is carried out in the turbulent flows, importance has to be given to transitional and turbulent flows.
- Nanoparticle distribution, double-diffusive, Soret, Dufort, chemical reactions can be incorporated into the study.
- Future research can be improved with non-linear convection, non-linear radiation based studies.
- Bifurcation studies are also recommended.

## References

[1] Bejan A, Dincer I, Lorente S, Miguel AF, Reis AH. Porous and Complex Flow Structures in Modern Technologies [Internet]. New York, NY: Springer New York; 2004. Available from: http://link.springer.com/10.1007/978-1-4757-4221-3

[2] Vafai K. Handbook of Porous Media [Internet]. Vafai K, editor. Handbook of Porous Media. CRC Press; 2015. Available from: https://www.taylorfrancis.com/books/9781439885574

[3] Prasad AK, Koseff JR. Combined forced and natural convection heat transfer in a deep lid-driven cavity flow. Int J Heat Fluid Flow. 1996 Oct 1;17(5):460-7.

[4] Kandaswamy P, Muthtamilselvan M, Lee J. Prandtl number effects on mixed convection in a lid-driven porous cavity. J Porous Media [Internet]. 2008 [cited 2021 Mar 16];11(8):791–801. Available from: http://www.dl.begellhouse.com/journals/49dcde6d4c0809db,20e6af7e1c676c96,21713be21d71b6f0.html

[5] Lawrence J, Mohanadhas B, Narayanan N, Kumar AV, Mangottiri V, Govindarajan SK. Numerical modelling of nitrate transport in fractured porous media under non-isothermal conditions. Environ Sci Pollut Res [Internet]. 2021 Aug 7; Available from: https://link.springer.com/10.1007/s11356-021-15691-8

[6] Choi SUS, Eastman JA. Enhancing thermal conductivity of fluids with nanoparticles. ASME Internarional Mech

Eng Congr Expo [Internet]. 1995; Available from: httpswww.osti.govbiblio196525

[7] Das SK, Choi SUS, Patel HE. Heat transfer in nanofluids - A review. Heat Transf Eng. 2006;27(10):3-19.

[8] Gupta S, Kumar D, Singh J, Gupta S. Impact of generalized Fourier's law and Fick's law for MHD flow of Ag–H 2 O and TiO 2 –H 2 O nanomaterials. Multidiscip Model Mater Struct [Internet]. 2019 Nov 4;15(6):1075–99. Available from: https://www.emerald.com/insight/content/doi/10.1108/MMMS-12-2018-0216/full/html

[9] Gupta S, Kumar D, Singh J. Magnetohydrodynamic three-dimensional boundary layer flow and heat transfer of water-driven copper and alumina nanoparticles induced by convective conditions. Int J Mod Phys B [Internet]. 2019 Oct 20;33(26):1950307. Available from: https://www.worldscientific.com/doi/abs/10.1142/S0217979219503077

[10] Jino L, Kumar AV. MHD Natural Convection of Hybrid Nanofluid in a Porous Cavity Heated With a Sinusoidal Temperature Distribution. Comput Therm Sci An Int J. 2021;13(5):83-99.

[11] Ghasemi B, Aminossadati SM, Raisi A. Magnetic field effect on natural convection in a nanofluid-filled square enclosure. Int J Therm Sci. 2011;50(9):1748-56.

[12] Selimefendigil F, Öztop HF. Natural convection and entropy generation of nanofluid filled cavity having different shaped obstacles under the influence of magnetic field and internal heat generation. J Taiwan Inst Chem Eng. 2015 Nov 1;56:42-56.

[13] Selimefendigil F, Öztop HF, Chamkha AJ. MHD mixed convection and entropy generation of nanofluid filled lid driven cavity under the influence of inclined magnetic fields imposed to its upper and lower diagonal triangular domains. J Magn Magn Mater. 2016 May 15;406:266-81.

[14] Basak T, Roy S, Singh SK, Pop I. Analysis of mixed convection in a lid-driven porous square cavity with linearly heated side wall(s). Int J Heat Mass Transf [Internet]. 2010;53(9-10):1819-40. Available from: http://dx.doi.org/10.1016/j.ijheatmasstransfer.2010.01.007

[15] Basak T, Krishna Pradeep P V., Roy S, Pop I. Finite element based heatline approach to study mixed convection in a porous square cavity with various wall thermal boundary conditions. Int J Heat Mass Transf [Internet]. 2011;54(9-10):1706-27. Available from: http://dx.doi.org/10.1016/j.ijheatmasstransfer.2010.12.043

[16] Basak T, Roy S, Chamkha AJ. A Peclet number based analysis of mixed convection for lid-driven porous square cavities with various heating of bottom wall. Int Commun Heat Mass Transf [Internet]. 2012;39(5):657-64. Available from: http://dx.doi.org/10.1016/j.icheatmasstransfer.2012.03.022

[17] Yaghoubi Emami R, Siavashi M, Shahriari Moghaddam G. The effect of inclination angle and hot wall configuration on Cu-water nanofluid natural convection inside a porous square cavity. Adv Powder Technol [Internet]. 2018;29(3):519-36. Available from: https://doi.org/10.1016/j.apt.2017.10.027

[18] Wilkes JO, Churchill SW. The finite-difference computation of natural convection in a rectangular enclosure. AIChE J. 1966;12(1):161-6.

[19] Rudraiah N, Barron RM, Venkatachalappa M, Subbaraya CK. Effect of a magnetic field on free convection in a rectangular enclosure. Int

J Eng Sci. 1995;33(8):1075-84.

[20] Lawrence J, Alagarsamy VK. Mathematical Modelling of MHD Natural Convection in a Linearly Heated Porous Cavity. Math Model Eng Probl [Internet]. 2021 Feb 28;8(1):149-57. Available from: http://www.iieta.org/journals/mmep/paper/10.18280/mmep.080119

[21] Singh J, Rashidi MM, Sushila, Kumar D. A hybrid computational approach for Jeffery–Hamel flow in non-parallel walls. Neural Comput Appl [Internet]. 2019 Jul 30;31(7):2407-13. Available from: http://link.springer.com/10.1007/s00521-017-3198-y

[22] Sushila, Singh J, Kumar D, Baleanu D. A hybrid analytical algorithm for thin film flow problem occurring in non-Newtonian fluid mechanics. Ain Shams Eng J [Internet]. 2021 Jun;12(2):2297–302. Available from: https://linkinghub.elsevier.com/retrieve/pii/S2090447920302008

[23] Gupta S, Kumar D, Singh J. Analytical study for MHD flow of Williamson nanofluid with the effects of variable thickness, nonlinear thermal radiation and improved Fourier's and Fick's Laws. SN Appl Sci [Internet]. 2020 Mar 18;2(3):438. Available from: http://link.springer.com/10.1007/s42452-020-1995-x

[24] Grosan T, Revnic C, Pop I, Ingham DB. Magnetic field and internal heat generation effects on the free convection in a rectangular cavity filled with a porous medium. Int J Heat Mass Transf. 2009;52(5–6):1525-33.

[25] Revnic C, Grosan T, Pop I, Ingham DB. Magnetic field effect on the unsteady free convection flow in a square cavity filled with a porous medium with a constant heat generation. Int J Heat Mass Transf. 2011 Apr 1;54(9–10):1734-42.

[26] Rashad AM, Rashidi MM, Lorenzini G, Ahmed SE, Aly AM. Magnetic field and internal heat generation effects on the free convection in a rectangular cavity filled with a porous medium saturated with Cu–water nanofluid. Int J Heat Mass Transf [Internet]. 2017;104:878–89. Available from: http://dx.doi.org/10.1016/j.ijheatmasstransfer.2016.08.025

[27] Jino L, Vanav Kumar A. Fluid Flow and Heat Transfer Analysis of Quadratic Free Convection in a Nanofluid Filled Porous Cavity. Int J Heat Technol [Internet]. 2021 Jun 30;39(3):876–84. Available from: https://www.iieta.org/journals/ijht/paper/10.18280/ijht.390322

[28] Jino L, Kumar AV. Cu-Water Nanofluid MHD Quadratic Natural Convection on Square Porous Cavity. Int J Appl Comput Math [Internet]. 2021 Aug 24 [cited 2021 Jul 26];7(4):164. Available from: https://link.springer.com/article/10.1007/s40819-021-01103-5

[29] Kumar AV, Jino L, Berlin M, Mohanty PK. Magnetic field effect on nanofluid suspension cavity by non-uniform boundary conditions. In: AIP Conference Proceedings. AIP Publishing; 2019.

[30] Jino L, Vanav Kumar A, Maity S, Mohanty P, Sankar DS. Mathematical modeling of a nanofluid in a porous cavity with side wall temperature in the presence of magnetic field. In AIP Publishing; 2021. p. 020007–1--020007–8. Available from: http://aip.scitation.org/doi/abs/10.1063/5.0046109

[31] Jino L, Vanav Kumar A, Doley S, Berlin M, Mohanty PK. Numerical Modelling of Porous Square Cavity Heated on Vertical Walls in Presence of Magnetic Field. In: Mahanta P, Kalita P, Paul A, Banerjee A, editors. Advances in Thermofluids and Renewable Energy [Internet]. Springer, Singapore; 2022 [cited 2021 Nov 20]. p. 127–37. Available from:

https://link.springer.com/chapter/10.1007/978-981-16-3497-0_10

[32] Sivasankaran S, Mansour MA, Rashad AM, Bhuvaneswari M. MHD mixed convection of Cu–water nanofluid in a two-sided lid-driven porous cavity with a partial slip. Numer Heat Transf Part A Appl [Internet]. 2016 Dec 16 [cited 2021 Mar 17];70(12):1356-70. Available from: https://www.tandfonline.com/doi/abs/10.1080/10407782.2016.1243957

[33] Chamkha AJ, Rashad AM, Mansour MA, Armaghani T, Ghalambaz M. Effects of heat sink and source and entropy generation on MHD mixed convection of a Cu-water nanofluid in a lid-driven square porous enclosure with partial slip. Phys Fluids [Internet]. 2017 May 1 [cited 2021 Mar 17];29(5):052001. Available from: http://aip.scitation.org/doi/10.1063/1.4981911

[34] Sheikholeslami M. CuO-water nanofluid flow due to magnetic field inside a porous media considering Brownian motion. J Mol Liq [Internet]. 2018 Jan 1 [cited 2021 Mar 18];249:921-9. Available from: https://linkinghub.elsevier.com/retrieve/pii/S0167732217344057

[35] Çolak E, Ekici Ö, Öztop HF. Mixed convection in a lid-driven cavity with partially heated porous block. Int Commun Heat Mass Transf [Internet]. 2021 Jul;126:105450. Available from: https://linkinghub.elsevier.com/retrieve/pii/S0735193321003432